Aerospace Systems
https://doi.org/10.1007/s42401-024-00312-2

ORIGINAL PAPER

On the hysteretic response of mechanical strain induced by thermal stress in fastened metal-composite hybrid structures during a temperature cycle

Zhiyuan Cong[1,2] · Zhefeng Yu[1,2] · Dongjie Jiang[1,2]

Received: 27 February 2024 / Revised: 11 June 2024 / Accepted: 16 July 2024

Abstract
As the use of composite materials in aerospace is growing fast, more metal-composite hybrid structures come into being and thermal stress becomes increasingly a concern that may affect structural safety. In this paper, experimental and numerical studies are conducted on the mechanical strain induced by thermal stress in an AL/CFRP hybrid structure subjected to a heating–cooling–heating cycle. The studied hybrid structure consists of a metal plate and a composite laminate fastened by three bolts. The experimental results show that the mechanical strain in either metal or composite exhibits a hysteresis as the structure undergoes the temperature cycle, which implies the existence of structural nonlinearities. Finite element analysis, which incorporates details of the bolt joint, reproduces the hysteretic responses that reach a reasonable agreement with the experimental ones. Numerical studies disclose the effects of the structural parameters, i.e., friction coefficient, clamping force, fastener-hole clearance and bolt spacing, on the hysteresis and provide insights into the physical events during the thermal cycling. The reported work reveals that the movement of the bolts inside the surrounding holes is the key mechanism that drives the hysteretic thermal stress in the tested structure and sheds light on further investigations of structural safety of such hybrid structures under cyclic thermomechanical conditions.

Keywords Hybrid structure · Bolt · Thermal stress · Hysteresis · Finite element analysis

1 Introduction

Compared with metals, composite materials possess many excellent properties such as high specific strength and large specific modulus [1]. Therefore, more and more composite materials are used in aircrafts to reduce weight and improve flight performance while meeting strength requirements [2]. Composite materials were initially used for non-load-bearing parts, but now they are used in secondary and even primary load-bearing parts [3]. As composite materials find widespread applications across various fields, and metal materials retain unique and irreplaceable characteristics in certain structures, the emergence of metal-composite hybrid structures becomes inevitable. The main type of connection method used in these structures is mechanical connection [4], such as bolt joint, which is widely used in aerospace because of the high reliability [5]. Due to the large difference in coefficients of thermal expansion (CTEs) between the constituents, when the temperature changes, the metal and composite components in a hybrid structure will be mutually constrained and generate thermal stress even the structure is subjected to no external loading. In the field of aerospace, aircrafts usually undergo severe temperature changes during service, consequently thermal stress and its effects on the stress states in the components of metal-composite hybrid structures during thermal cycles cause concerns about structural safety.

A few studies have been reported on the experiment and analysis of the mechanical responses of hybrid structures which consist of components fastened by bolt joints. It is found that temperature changes will affect the internal load distribution and stress state in fastened hybrid composite/aluminum structures. Yang [6] studied the interaction

✉ Dongjie Jiang
jiang-xia@sjtu.edu.cn

1 Lab of Civil Aircraft Structures Testing, School of Aeronautics and Astronautics, Shanghai Jiao Tong University, Shanghai 200240, China

2 Aerospace Structure Research Center, School of Aeronautics and Astronautics, Shanghai Jiao Tong University, Shanghai 200240, China

Published online: 03 August 2024

between the Z-shaped aluminum beams and the solid composite laminate in a bolted hybrid structure, that is part of an aircraft's fuselage. The experiments showed that for the multi-bolt hybrid structure, the end bolts bear greater shear loads than the intermediate bolts when the temperature changes and a theoretical model was established to analyze the thermal stress in metal-composite hybrid structures and produced results that fit well with the experimental results. Deng [7] used a finite element model to simulate Yang's experiments and drew the same conclusion as Yang's. Wei [8] employed ABAQUS to simulate a metal-composite hybrid structure, in which a uniform temperature field is applied to the model and the rigid displacement is constrained. They found that the greater the difference between the initial assembly temperature and the operating temperature, the greater the load on the connecting bolts. Temperature also affects the stiffness and strength of fastener joints. Experiments have shown that the strength of the joint is affected by temperature, whether it is a single-lap double-fastener joint or a double-lap single-bolt joint. At room temperature, the strength and stiffness of the joint are higher than those at high temperatures [9–13].

In addition, scholars have also conducted research on theoretical models. Finite element simulations of fastened metal-composite hybrid structural joints typically ignore the compliance of the fasteners and therefore produce relatively conservative thermal stress and strain results. In order to solve this problem, Norwood [14] developed a theoretical model to correct the finite element model of the rigid connection between the skin and spar nodes to obtain more accurate thermal strains. Through static tensile experiments, Zhu [15, 16] found that high temperature will affect the failure mode of screwed single-lap CCF300/AC721-30CrMnSiA joint and proposed a progressive damage model (PDM) based on damage criteria and temperature effects. Coman et al. [17] investigated countersunk-bolted aluminum–composite joints and developed a PDM for this hybrid structure which considered all the nonlinearities such as geometric, material and friction-based full contact. They found that as the temperature increased, the failure mode of the structure changed from net section failure to bearing failure and even shear failure. This is because at low temperatures, the material becomes more brittle. At high temperatures, the plasticity of the material increases, and a significant yielding process is observed before ultimate failure. Experiments have proven that high temperature and humidity can affect the fatigue life of joints. In combination with experimental analysis of joint failure modes, Karimi [18] conducted the first study on the impact of hygrothermal aging on the static strength and fatigue three-point bending strength of AL/CFRP single-lap joints. Zhu [19] proposed a temperature-humidity-mechanical coupled fatigue behavior evaluation method. This model can simulate the fatigue failure mechanism and mode of threaded composite-metal joints in any temperature-humidity environment and predict their fatigue life.

Existing studies mainly focus on the effects of temperature on the strength, stiffness and fatigue performance of joints in fastened structures. However, few work is reported on the thermal stress in fastened metal-composite hybrid structures, especially its evolution with temperature change and how it is affected by the structural parameters of fastening, which are fundamental problems for future studies on the thermal fatigue of such structures. In this article, we perform experiments to measure the mechanical strain induced by thermal stress in a bolted metal-composite hybrid structure subjected to a heating–cooling–heating cycle, and analyze numerically by finite element modeling to explore the mechanism behind the measured responses and the effects of fastening parameters. Section 2 elaborates the setup and results of the experimental work. Section 3 describes the finite element model, the comparison between the simulation and experimental results and the impacts of several fastening parameters such as friction coefficient, clamping force, fastener-hole clearance and bolt spacing on the hysteretic response. Conclusions are drawn in Sect. 4.

2 Experiment

Experimental tests were conducted on bolted metal-composite hybrid structures subjected to a heating–cooling–heating cycle.

2.1 Specimens

Figure 1a shows the schematic of a specimen and its detailed geometric dimensions are illustrated in Fig. 1b. A specimen consists of a metal plate and a composite laminate, with the same width of 28.56 mm. The thicknesses of the metal plate and the composite laminate are 2.70 mm and 4.56 mm, respectively. The overlap of the two components is 218.96 mm long and fastened by three bolts along the longitudinal centerline with a spacing of 95.20 mm. The nominal diameter of the bolt is 4.80 mm. Strain gauges are attached on the surface at the midpoints between neighboring bolts in order to measure the mechanical strain induced by thermal stress. The locations of the strain gauges are named Site #1–4, as highlighted in the figure. Six specimens manufactured in the same batch were tested in the experiment, and the data acquired were analyzed statistically to check the confidence of the results.

A composite laminate consists of 24 unidirectional carbon fiber reinforced polymer (CFRP) plies with a stacking sequence of [45/0/-45/90]3S. The matrix of the composite is epoxy resin. Each ply has a thickness of 0.19 mm and the total thickness of the laminate is 4.56 mm. The elastic

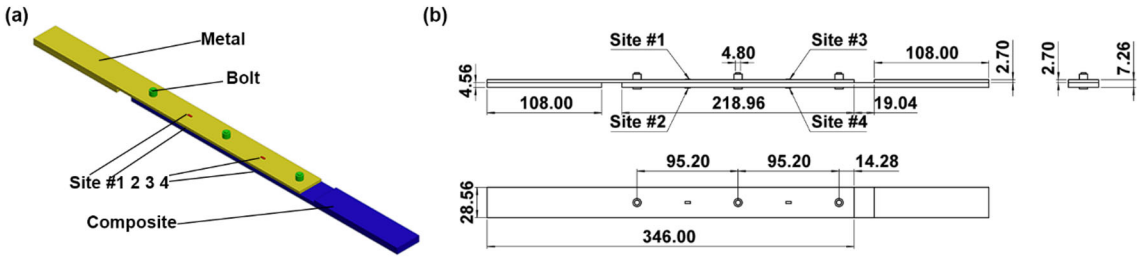

Fig. 1 The **a** schematic and **b** geometric dimensions of a specimen

Table 1 Material properties

Property	Material		
	Lamina	Al	Ti
E_1 (GPa)	144.5	72.4	110.24
E_2 (GPa)	8.25		
E_3 (GPa)	8.25		
ν_{12}	0.32	0.33	0.33
ν_{13}	0.32		
ν_{23}	0.32		
G_{12} (GPa)	4.5	27.218	41.444
G_{13} (GPa)	4.5		
G_{23} (GPa)	4.5		
$\alpha_{11}(10^{-6}/°C)$	0.15	23.04	8.82
$\alpha_{22}(10^{-6}/°C)$	28.7		
$\alpha_{33}(10^{-6}/°C)$	28.7		

constants and CTEs for each ply in the material principal coordinate system are measured separately and shown in the second column in Table 1. One may note that the laminae are orthotropic and the symmetric stacking sequence makes the laminate orthotropic. The material of the metal plate is an aluminum alloy of grade 7050-T7451 with the material specification AMS4050. The bolt is made by titanium alloy of grade Ti-6AL-4V-annealed, and the material specification is AMS4911. The bolt model is CFBL1001AG6, the nut model is CFNT1003CY6, and the nominal diameter of the bolt is 4.76 mm. The Young's modulus, Poisson's ratio and CTE of the aluminum alloy and titanium alloy are listed in the third and fourth columns of Table 1.

2.2 Measurement method of the mechanical strain induced by thermal stress

In the experiment, no external loads are exerted on the specimens, which are only subjected to temperature changes. Given the inherent challenges associated with directly measuring thermal stress, the mechanical strain ε^M induced by thermal stress is quantified in this study using strain gauges. The reading of a strain gauge ε^S attached on a specimen can be divided into:

$$\varepsilon^S = \varepsilon^M + \varepsilon^T. \tag{1}$$

In Eq. (1), ε^T is termed *thermal output* and includes the following terms [20]:

$$\varepsilon^T = \left[\frac{\alpha_g}{K} + \left(\beta_s - \beta_g\right)\right]\Delta T \tag{2}$$

where α_g is the temperature coefficient of electric resistance of the gauge material, K is the sensitivity factor of the strain gauge, β_s and β_g are the CTEs of the specimen and gauge materials respectively, and ΔT is the change in temperature. In Eq. (2), the first term $(\alpha_g/K)\Delta T$ represents the change of electric resistance of the gauge solely caused by temperature change and $(\beta_s - \beta_g)\Delta T$ stands for the interaction between the specimen and the gauge due to the mismatch of their CTEs. One should note that all coefficients in Eq. (2) may be functions of temperature, rather than constants. Equation (2) indicates that the thermal output includes not only the thermal expansion of the specimen, but also complicated additional terms related to the gauge material.

It can be easily seen from Eq. (1) that the mechanical strain induced by thermal stress ε^M can be extracted by subtracting the thermal output from the strain gauge reading. The relation between the thermal output ε^T and temperature change ΔT is usually nonlinear and even complex. Rather than curve fitting this relation by polynomials like [6], we utilize coupon samples of the aluminum alloy and the composite laminate, fabricated concurrently with those employed in specimen assembly, adhering to a consistent batch. The coupons are 75 mm long and 55 mm wide and the length direction is parallel to the longitudinal direction of the specimens. The thickness of the composite coupon is the same as the composite laminate in the specimen, and the thickness of the metal coupon is 4 mm. In the experiment, the coupons are placed in a free-standing manner in the same environment with the specimens, and resultantly the reading of any strain gauge on the coupons is the thermal output since no mechanical load is applied or generated. Four strain gauges are attached onto each coupon along the length direction, and

their mean reading is taken to be the thermal output ε^T used to extract the mechanical strain.

A specimen is fabricated through joining a composite laminate and a metal plate by bolts, and thus the reading of a strain gauge on the specimen ε^S includes both mechanical strain induced by thermal stress ε^M, which is generated because of the mismatch between the CTEs of the composite and the metal, and thermal output ε^T, which is related to temperature change by Eq. (2). A coupon, either composite or metal, subjected to temperature change exhibits only thermal output ε^T described by Eq. (2) and does not incur mechanical strain because it is neither loaded nor fastened to other structures. For data processing, the mechanical strain at a gauged site on a specimen is calculated by subtracting the thermal output ε^T of the coupons made by the same material from the local strain gauge reading.

2.3 Experiment scheme

The setup and scheme of the experiment are illustrated in Fig. 2. The interior temperature of the environmental chamber can be controlled electronically. Signals from all strain gauges are transmitted into an MTS dynamic data acquisition system. A thermocouple is adhered to each surface of the specimens and the coupons on which strain gauges are attached, in order to monitor the temperature of the tested structures. Figure 3 shows photos of the equipment and specimens/coupons. The specimens are placed freely in the chamber and wood blocks are used to keep them stand in the vertical direction, in order to avoid interacting with each other. The coupons are placed separately on a steel web.

The experiment involves five types of environments with different temperature values, as shown in Table 2. The complete temperature history in the experimental cycle is RT → ETD1 → ETD2 → ETD1 → RT → LTD1 → LTD2 → LTD1 → RT, as shown by the plot at the left bottom corner in Fig. 2. At each temperature point, the temperature of the environmental chamber is set to the target value and its climate control system starts to adjust the interior environment. When the readings of all thermocouples lie within ± 2 °C around the target temperature and keep unchanged for more than 5 min, the data of strain gauge readings are collected and then the experiment proceeds towards the subsequent temperature point.

2.4 Experiment result

As stated in Sect. 2.2, the mechanical strain induced by thermal stress ε^M on the surface of a metal plate or a composite laminate in a specimen can be calculated as

$$\varepsilon^M = \varepsilon^S - \varepsilon^T, \tag{3}$$

where ε^S is the reading of the strain gauge attached on the specimen, and ε^T is the mean reading of the strain gauges on the coupon made with the same material with the gauged component of the specimen.

The responses of thermal stress-induced mechanical strain ε^M versus temperature measured at the four gauged sites in Fig. 1 are plotted in Fig. 4. The solid dots are the average of the measured values at the same site on the six specimens and the error bars are determined from the standard errors. Smaller error bars suggest that the test results of the six specimens have a higher level of confidence. The mechanical strain–temperature curve at Site #1 or #3, which is on the surface of the metal plate, possesses a positive slope generally. On the contrary, the curve on the surface of the composite, i.e., Site #2 or #4, has a negative slope. It is interesting to find that the mechanical strain on either the metal or composite sides exhibits a hysteresis loop as the temperature undergoes the heating–cooling–heating cycle. On the metal plate, e.g., at Site #1, the difference of the mechanical strains at 71 °C, i.e., bullets ② during heating and ④ during cooling, is 45.2 με (1 $\mu\varepsilon = 10^{-6}$). In the process of cooling, the temperature passes through RT at bullet ⑤ with a residual mechanical strain of − 51.1 με. In the temperature range below RT, the difference of the mechanical strains at − 25 °C (bullets ⑥ during cooling and ⑧ during heating) is 78.0 με. At the end of the experiment (bullet ⑨), the hysteresis loop is not closed, with a residual mechanical strain of 39.1 με. On the composite laminate, e.g., at Site #2, the difference of mechanical strain is 110.1 με at 71 °C between bullets ② and ④ and 110.5 με at − 25 °C between bullets ⑥ and ⑧. The residual strain at RT is 139.3 με and − 100.1 με at bullets ⑤ and ⑨ respectively. The mechanical strain-temperature hysteresis at Site #1 encloses an area of 8175 με °C and the hysteresis at Site #2 encloses an area of 17,645 με °C. The mechanical strain responses at Sites #3 and #4 are quite close to those at Sites #1 and #2, indicating that the specimen is essentially symmetric about the central bolt.

3 Numerical result and discussions

A finite element (FE) model has been developed to simulate the bolted metal-composite hybrid structure subjected to the heating–cooling–heating cycle, to investigate the cause of the hysteretic response of thermal stress and reveal the effects of various structural parameters on the hysteresis.

3.1 Finite element model

The finite element model of the hybrid structure incorporating the nonlinearity induced by contact, is shown in Fig. 5. The metal plate, composite laminate and bolts are modeled according to the actual geometric dimensions of

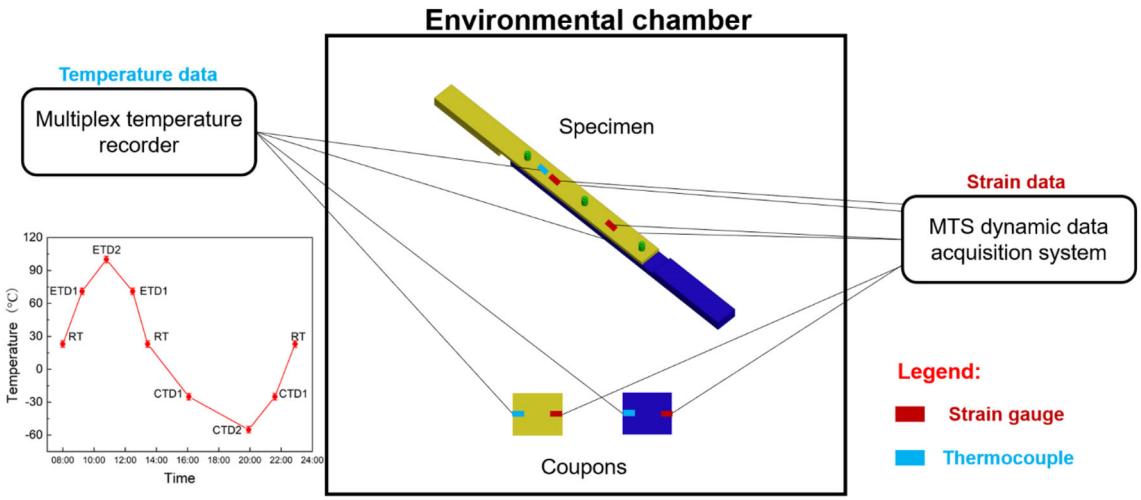

Fig. 2 Schematic of the experimental setup and scheme of thermal loading

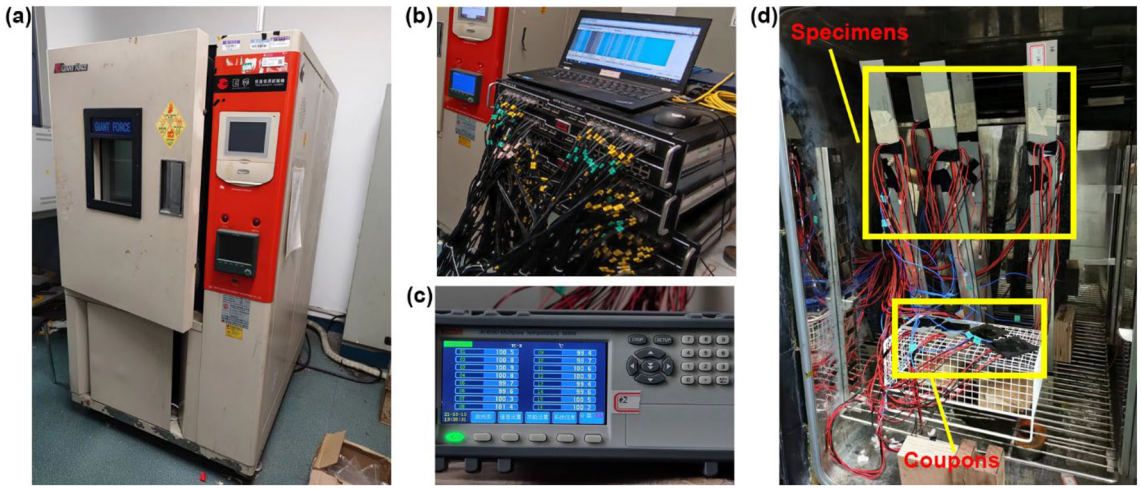

Fig. 3 **a** The environment chamber; **b** the MTS dynamic data acquisition system; **c** multiplex temperature recorder; **d** specimens and coupons placed inside the environment chamber before testing

Table 2 Experimental temperatures

Environment name*	Target temperature (°C)	Tolerance (°C)
RT	26	± 2
LTD1	− 25	± 2
LTD2	− 55	± 2
ETD1	71	± 2
ETD2	100	± 2

*RT = room temperature, LTD = low temperature and dry, ETD = elevated temperature and dry

the specimens and discretized by using three dimensional reduced-integration solid elements C3D8R in the software ABAQUS®. This type of element is employed to reduce the computational cost. In the direction through the thickness, there are 8 elements in the metal plate and 24 elements in the composite laminate. Note that each ply of the laminate is meshed by a layer of elements, and the orientation of the ply is prescribed according to the stacking sequence described in Sect. 2.1. In the plane parallel to the surfaces, a structured mesh with square elements with the size of 2.38 mm is used to discretize the region far from the holes, while the element size on the peripheral of the holes is 0.32 mm (totally 48 elements around the hole peripheral) and a transition zone exist between the two mesh densities, as shown by the right bottom inset in Fig. 5. Each bolt is meshed with a density such that the element size on its surface is the same with the elements on the peripheral of the holes in the metal or composite plates, where they contact potentially. The adopted mesh is chosen based on the sensitivity studies of the simulation results on mesh density, as presented in Appendix. Note that there is a

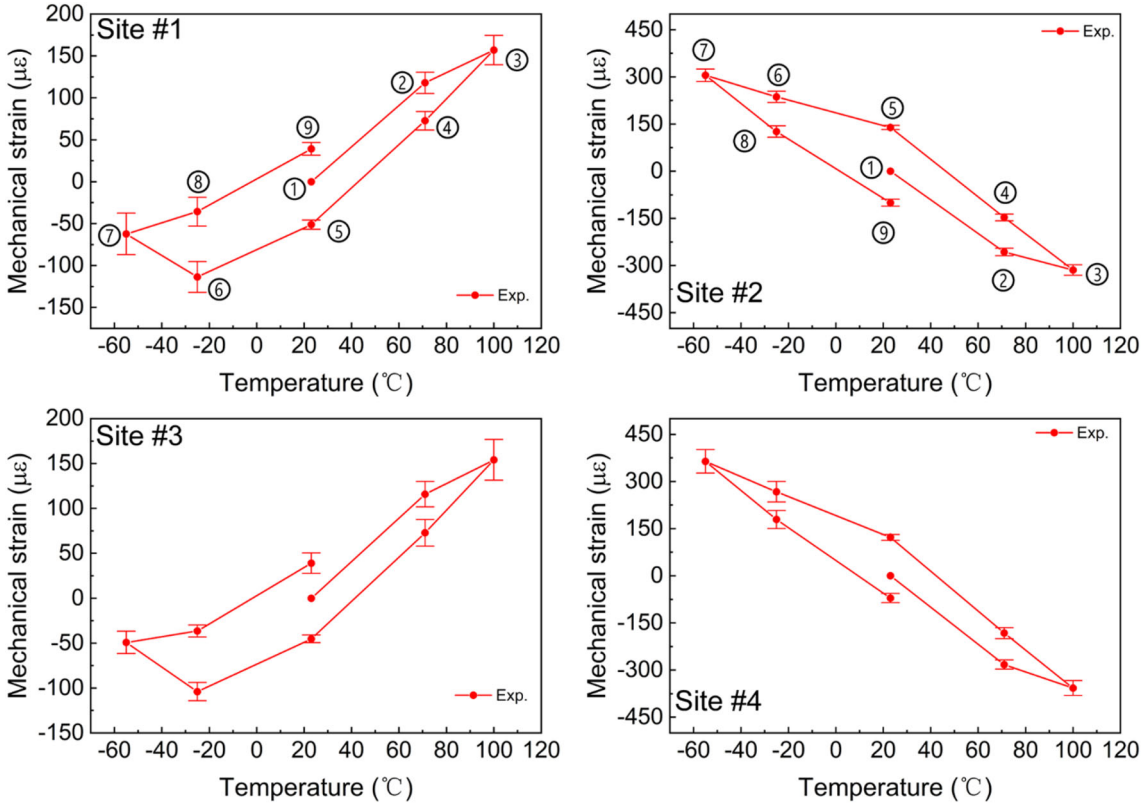

Fig. 4 Experimental results of the mechanical strain induced by thermal stress at the four gauged sites during the temperature cycle

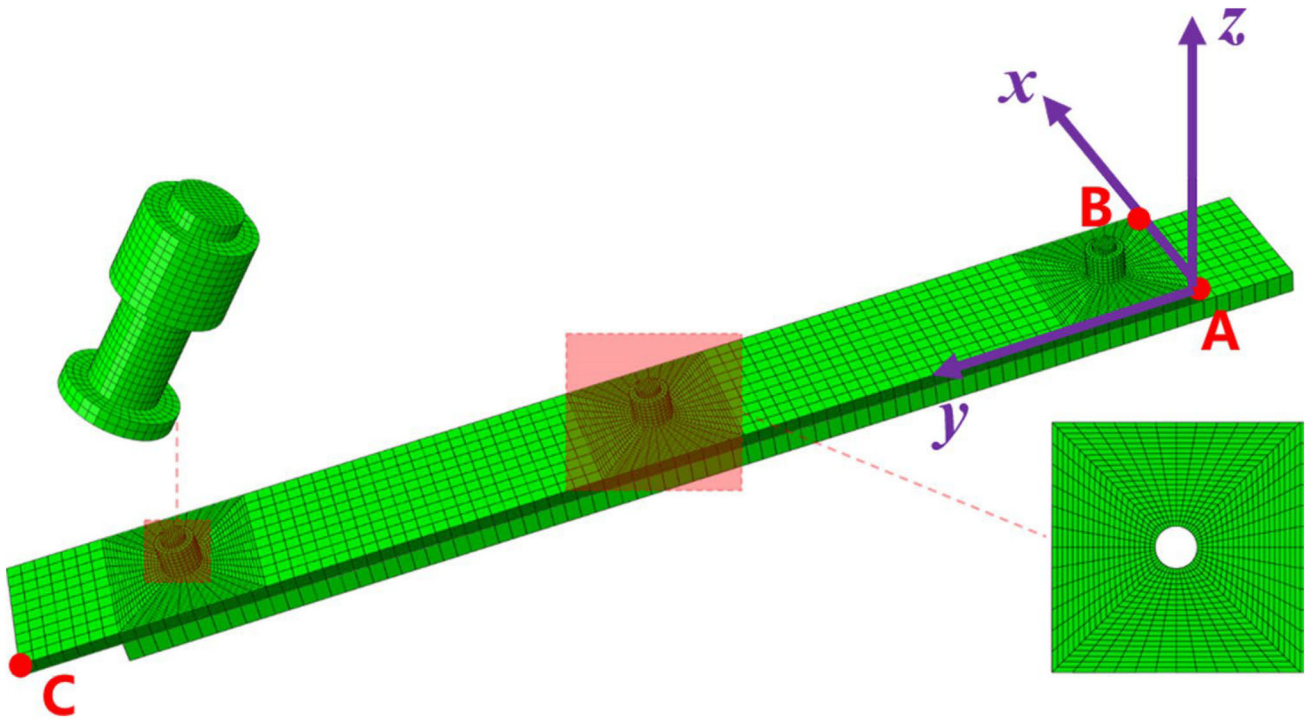

Fig. 5 Schematic of the finite element model

gap between the bolt and the screw hole, which is termed as fastener-hole clearance. Note that the hole diameter on the specimen is 4.86 mm, while the bolt diameter is 4.80 mm, resulting in an initial clearance of 0.03 mm between a bolt and its hole.

The elastic constants for the aluminum alloy, composite plies and titanium alloy as shown in Table 1 are assigned to corresponding parts in the FE model. All pairs of surfaces that may contact with each other are assigned a contact property, in which "hard contact" is assumed in the normal direction and the tangential behavior abides by the Coulomb friction model with a friction coefficient of 0.1. Each bolt is assigned an initial clamping force or preload of 3000 N, and its length is assumed to be fixed in the process of heating or cooling, leaving the clamping force to evolve. The preload force is applied to the middle surface of the screw. When the temperature increases, the bolt should expand, but due to the choice of fixed bolt length, the preload force is increased at this time. The opposite is true when the temperature decreases. The specimens are unconstrained in the experiment, thus in the simulations we eliminate the rigid body motion of the model without any unnecessary constraint that may bring additional loadings. In the coordinate system in Fig. 5, all three translational displacements at point A, the translational displacements in y and z directions at point B, and the z displacement at point C are constrained. The simulation is performed in a step of static analysis in which the whole model is assigned a spatially uniform temperature field evolving according to the experimental scheme shown in Fig. 2.

There are other factors that potentially affect the hysteresis such as creeping of the constituent materials. However, creeping is neglected in this work because the stress inside the composite laminate or metal plate, approximated by elastic modulus times the measured local mechanical strain, is in the order of 10 MPa, which is too small for creeping to play a significant role during the timescale of the test. This is also evidenced by the stability of experimental data when the temperature in the chamber is kept. Consequently, the hysteretic response is mainly attributed to the structural nonlinearities induced by fastening in the FE model.

3.2 Simulation results

The simulated responses of mechanical strain versus temperature at the four gauged sites in the structure are plotted in Fig. 6 together with the experimental results. It can be seen that the hysteretic responses of the mechanical strain induced by thermal stress is reasonably reproduced. The simulated responses trace hysteretic loops similar to the experimental ones and exhibit the same trend of lagging when the temperature change switches between heating and cooling. The hysteresis on the metal side at Sites #1 and #3, is apparently more significant than that on the composite side at Sites #2 and #4. However, the magnitude of mechanical strain on the composite side is much higher than that on the metal side, similar to the experimental observations. The simulated hysteresis at Sites #1 and #2 enclose an area of 4520 με °C and 18,259 με °C, respectively. While the enclosed area at Site #1 is significantly lower than the experimental value of 8175 με °C, the enclosed area at Site #2 is quite close to the experimental measurement of 17,645 με °C.

We admit that there are some distinct differences between the simulated and experimental results, which is not surprising since it is almost impossible to reproduce everything in reality accurately in modeling. For example, the material properties presented in Table 1 are measured at RT but they may vary as the temperature changes. The contact behavior defined in the FE model is an over-simplified model and may be completely different from the actual case. In addition, the assumption that the initial states of the bolts are identical may also be too ideal. However, it is not our purpose to reproduce the experiment quantitatively. In the subsequent section, we will perform more FE analysis to reveal the impacts of various structural parameters on thermal stress and demonstrate that incorporation of the nonlinearities associated with the fastening, contact, and relative motion of bolts and holes, successfully explains the hysteresis phenomenon observed in the experiment.

3.3 Parametric studies

In this section, an attempt is made to study the effects of several structural parameters on the hysteresis phenomenon of mechanical strain induced thermal stress in the metal-composite hybrid structure. The following parameters are investigated: friction coefficient, clamping force, fastener-hole clearance and bolt spacing. The "benchmark" values of these parameters used in the FE analysis presented in Sect. 3.1 are summarized in Table 3. When analyzing the effect of a particular structural parameter, its value is changed and other parameters maintain their benchmark values.

(1) Friction coefficient

The configuration of the tested metal-composite hybrid structure contains many contact pairs, which is expected to be the major source of nonlinearities when the temperature changes. The tangential behavior in the contact definition is assumed to obey the Coulomb friction model, which is characterized by the friction coefficient μ. In this section, the influence of the friction coefficient on the mechanical strain hysteresis phenomenon is studied.

Five typical friction coefficients 0.01, 0.05, 0.1, 0.15, and 0.2 are considered in the FE analysis and the simulation results are plotted in Fig. 7. Because the mechanical strain on the

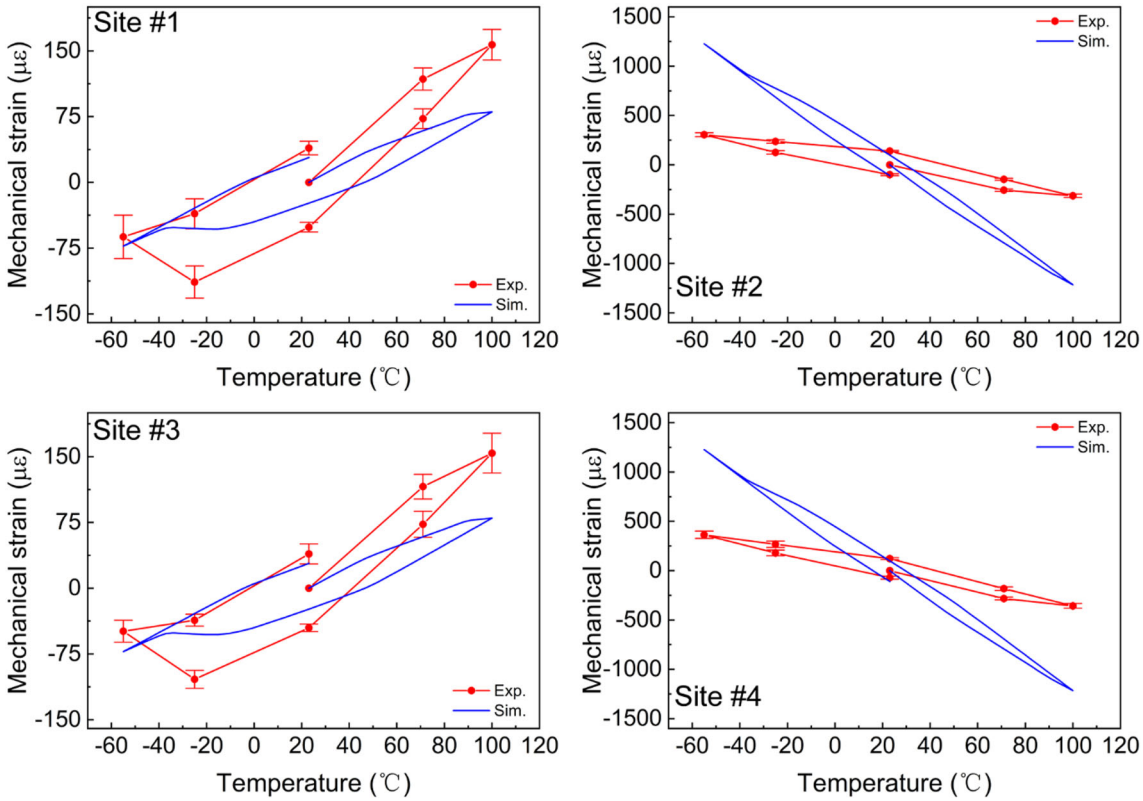

Fig. 6 Comparison of simulation and experimental results

Table 3 Structural parameters

Friction coefficient	Clamping force (N)	Fastener-hole clearance (mm)	Bolt spacing (mm)
0.1	3000	0.03	95.2

metal side is smaller in magnitude than that on the composite side, the hysteresis at Sites #1 and #3 is more noticeable. Let us take the mechanical strain at Site #1 as an example. For the friction coefficient $\mu = 0.01$, the mechanical strain response has an evident plateau under temperatures between − 15 and 60 °C during either heating or cooling and becomes almost linear for temperatures above 60 °C or below − 15 °C, similar to a typical hysteresis of ferroic materials [21, 22]. Compared to the case with $\mu = 0.01$, the slope of the mechanical strain-temperature curve increases when $\mu = 0.05$, and a larger temperature difference is required to enter the plateau and linear phases. For $\mu = 0.05$, the mechanical strain-temperature response becomes almost linear when the temperature is below − 28 °C or above 75 °C. At the same time, the temperature range corresponding to the plateau contracts. For friction coefficients of 0.1 and higher, the nearly flat plateaus disappear and the hysteresis loop gradually thins. The area enclosed by the hysteresis is 688, 2832, 4520, 3429, and 3037 με °C as the friction coefficient increases from 0.01 to 0.20, which displays a non-monotonic tendency.

It is extremely difficult to acquire the actual value of the friction coefficient and the value 0.1 is selected as the "benchmark" value in the FE model in Sect. 3.2 because it produces a result that is the closest to the experimental one.

Drawing insights from the FE simulations depicted in Fig. 7, one may deduce the physical events taking place in the metal-composite hybrid structure fastened by bolts throughout the heating–cooling–heating cycle. A bolt tightens the constituent plates by the clamping force, as well as by frictional forces between the contact pairs, such as those between the constituent plates and those between a plate and its neighboring nut or bolt head. Nonetheless, these frictional forces cannot entirely eliminate the relative movement between the bolt and the hole in the longitudinal direction of the structure. This movement dominates the shape and magnitude of the mechanical strain hysteresis caused by thermal stress, a topic that will be further elaborated in the following.

Figure 8a shows the hysteresis of mechanical strain on the metal side simulated with friction coefficient $\mu = 0.01$ (see also Fig. 7), together with the variation of the distance d_1 between Point P1 on the peripheral of the leftmost hole in Fig. 1 and its closest counterpart on the bolt surface, and a similar distance d_2, as depicted in Fig. 8b. This case is

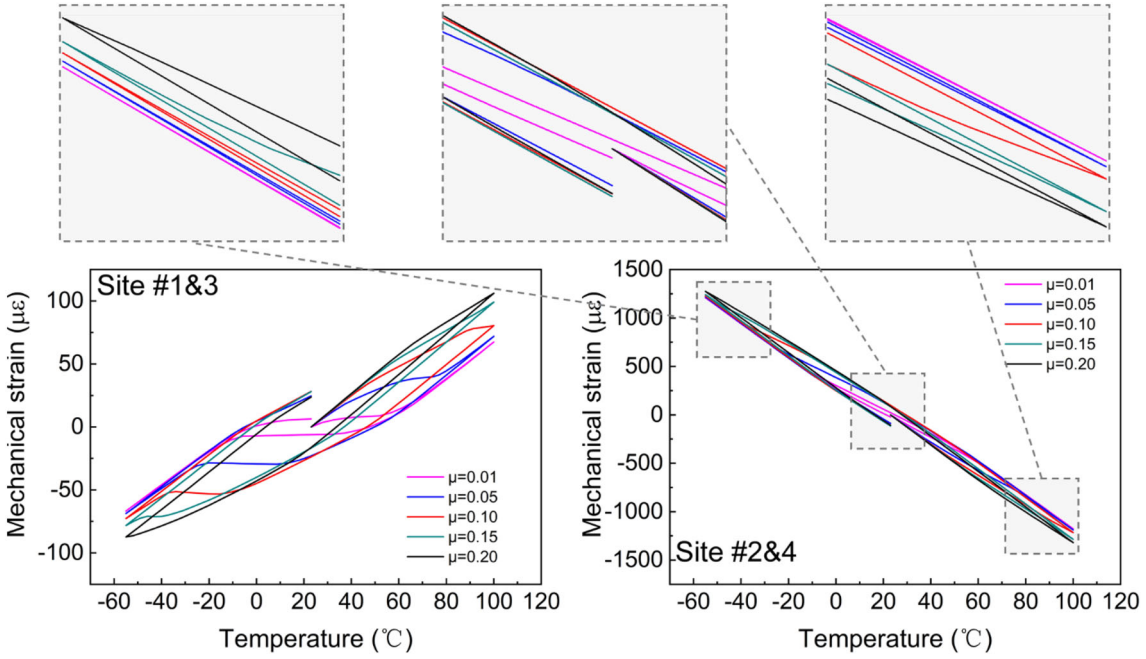

Fig. 7 Mechanical strain variation with temperature for different friction coefficients

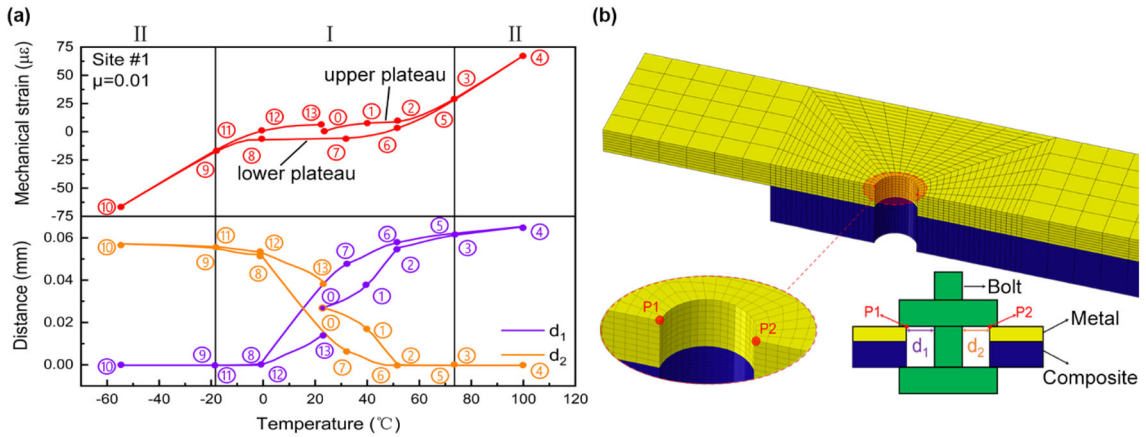

Fig. 8 **a** The mechanical strain of Site #1 and the fastener-hole distances d_1 and d_2; **b** the interested points and the definition of the distances

selected to study in detail because it is representative as such a small friction coefficient facilitates sliding between the contact pairs, as well as the relative movement of the bolt and hole. In the FE model, the nominal diameters of the bolt and the hole are 4.80 mm and 4.86 mm, resultantly $d_1 = d_2 =$ 0.03 mm in the initial state. After the initial clamping force is applied, d_1 and d_2 become 0.027 mm at bullet 0 due to Poisson's effect. As the temperature rises from bullet 0 to ②, the mechanical strain increases and gradually enters a plateau about 8.32 με, while the distance d_1 keeps growing and d_2 keeps dropping, which indicates that the bolt is moving inside the hole towards Point P2. The upper plateau has a rather small slope of 0.0935 με/°C.

The bolt comes into contact with the hole near ② where d_2 is nearly zero, after which the slope of the mechanical strain-temperature curve becomes steep and the increase of d_1 slows down. After bullet ③, the behavior of the structure becomes essentially thermoelastic, evidenced by reversibility of the responses of d_1, d_2 and the mechanical strain during heating along ③④ and those during the initial stage of cooling (④⑤). One should note that only two points are monitored here and the fact d_2 reaches zero at ② does not mean the bolt and the hole get into full contact immediately. Actually the contact area continues spreading after ② and saturates around ③. The cooling process from ⑤ to ⑥ produces the responses of mechanical strain and distance d_1 that exhibit lagging from those in the same temperature range during heating (②③).

This is because, during this process, the components of the structure exhibit a state of motion opposite to that during ②③, leading to a switch in the direction of internal frictional forces and consequently a lag of response.

From bullet ⑥, the distance d_2 starts to grow from zero and d_1 continues declining, which means that the bolt detaches from Point P2 and begins to move towards P1, while the mechanical strain response softens further and enters a lower plateau about − 5.66 με around bullet ⑦. The relative movement of the bolt goes on as the mechanical strain traces the lower plateau. The slope of the lower plateau (0.0436 με/°C) is also very small. The bolt movement stops again at bullet ⑧, where d_1 reaches zero and Point P1 gets into contact with the bolt surface. The subsequent process from ⑧ to ⑬ is similar to ②–⑦. It involves thermoelastic cooling and heating along ⑨–⑩–⑪, as well as the difference between the responses along ⑧⑨ and ⑪⑫due to the switch of friction direction. At the end of the cycle (bullet ⑬), the mechanical strain has returned to the upper plateau. Overall, the whole cycle can be divided into two types of regimes, as shown in Fig. 8a. Regime I is associated with the relative movement between the bolts and holes, and Regime II is thermoelastic as the bolts and holes maintain full contact.

Let us return to the effect of friction coefficient μ shown in Fig. 7. When the friction coefficient μ increases, it becomes more difficult for the bolts to move inside the holes, a trend can be observed that this bolt movement demands larger magnitude of temperature change (of Regime I) to drive. Regime I covers approximately the temperature range [− 18 °C, 74 °C] for $\mu = 0.01$ and [− 40 °C, 88 °C] for $\mu = 0.05$. As μ rises further to 0.10, 0.15, and 0.20, the upper limit for the temperature range of Regime I exceeds 100 °C and the lower limit drops to − 49 °C for $\mu = 0.10$ and some values below − 55 °C for $\mu = 0.15$ and 0.20, which indicates that Regime II at high temperature is not reached for the three cases and Regime II at low temperature is out of the tested range for $\mu = 0.20$. The disapperance of Regime II implies that the bolts do not come into full contact with the holes. One may also notice the second trend that widening of the temperature range of Regime I is associated with more significant variation of the mechanical strain magnitude. The slope of the mechanical response grows as the friction coefficient μ becomes larger. It is within expectation because higher thermal stress is generated to overcome the higher frictions. In addition, both the upper and lower plateaus narrow down and even disappear with the increase of friction coefficient.

The hysteretic responses of the mechanical strain induced by thermal stress look similar to the electrical/magnetic/mechanical hysteresis loops of ferroelectric/ferromagnetic/ferroelastic materials subjected to cyclic driving forces. For the metal-composite hybrid structure studied in this paper, the nonlinearities related to the relative movement between bolts and holes, the contact and friction on the contacting surfaces play a role analogous to the spontaneous polarization/magnetization/phase transformation in ferroic materials that are responsible for the hysteresis.

(2) Clamping force

In the assembly process of a specimen, a torque was applied to fasten the bolts, causing a force inside each bolt that clamps the metal plate and the composite laminate tightly. The magnitude of clamping force certainly affects the interactions between the constituent parts in the hybrid structure. In this section, we consider five values of clamping forces: 4500 N, 3500 N, 3000 N, 2500 N, and 1500 N, in which 3000 N is the designed clamping force in the actual structure. The results of FE simulations using these values are shown in Fig. 9. Let us take Site #1 as an example. The calculated mechanical strain-temperature responses clearly exhibit similar trends to the effects of increasing friction coefficient shown in Fig. 7, including widening of the temperature range of Regime I and diminishing of Regime II, as well as the non-monotonic change of enclosed area.

(3) Fastener-hole clearance

The size of the fastener-hole clearance δ, which is equal to d_1 or d_2 in the unfastened state in Fig. 8b, directly affects the contact relationship between the bolts and holes. As described before, the benchmark value of δ is 0.03 mm. Additional FE models of the metal-composite hybrid structure with bolt diameters of 4.60, 4.76, 4.84, and 4.86 mm are established while the hole diameter is kept at 4.86 mm and consequently the additional models have fastener-hole clearances of 0.13, 0.05, 0.01, and 0.00 mm, correspondingly.

The results of the FE simulations with variation of the fastener-hole clearance are shown in Fig. 10. In the range of 0–0.03 mm, the fastener-hole clearance has a significant impact on the hysteresis phenomenon. For fastener-hole clearances of 0.00, 0.01, and 0.03 mm, the area enclosed by the mechanical strain hysteresis at Site #1 consistently increase with the increment of clearance, starting from 610 με °C. In this range, as the fastener-hole clearance increases, the hysteretic curve of the mechanical strain induced by thermal stress widens. One should note that for zero clearance, the mechanical strain still exhibits a hysteresis, although rather slender, since the contact area between bolts and holes may grow and decay due to deformations.

For fastener-hole clearances of 0.05 and 0.13 mm, the enclosed area at Site #1 is 4135 and 4033 με °C and more importantly, the hysteretic responses simulated by these two values of clearance are essentially identical. It indicates that, the hysteresis on the metal side has saturated and further elevating the fastener-hole clearance would no longer influence the hysteresis. According to the insights provided by the discussions of bolt movement, it can be inferred that the fastener-hole clearances of 0.05 and 0.13 mm are larger than the space in which the bolt moves through and therefore the

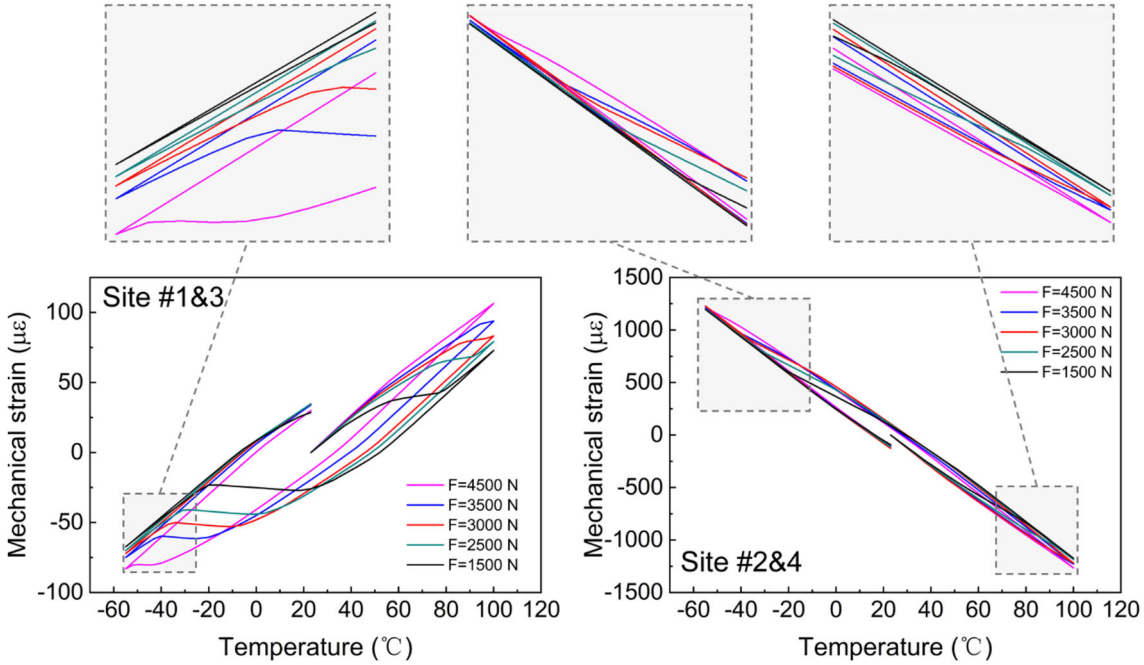

Fig. 9 Mechanical strain variation with temperature for different clamping force in specimen

screw of the bolt does not come into contact with the bolt at all in the whole cycle.

(4) Bolt spacing

For multi-bolted structures, the bolt spacing, denoted as L, is a structural factor that may influence the stiffness, strain distribution, and load distribution and transmission of the structure. Therefore, we consider five different bolt spacings, i.e., 105, 100, 95.2, 90 and 85 mm. Note that 95.2 mm corresponds to the specimens that underwent testing. The results of the FE simulations with these bolt spacing values are shown in Fig. 11. The area enclosed by the mechanical strain hysteresis at Site #1 decreases from 4603 to 4164 με °C as the bolt spacing increases from 85 to 105 mm. A trend can be observed that the hysteresis becomes a little more obvious as the bolt spacing decreases. Nevertheless, the influence of bolt spacing on the hysteresis is quite slight, which is attributed to the facts that the bolt movement is a localized event constrained inside the hole, whereas the studied values of bolt spacing are all much larger than the hole diameter. The effect of bolt spacing may be more evident if it is comparable to the hole diameter but this is out of the scope of our paper and will be addressed in future work.

4 Conclusion

In this article, the mechanical strain induced by thermal stress in a type of bolt-fastened metal-composite hybrid structure subjected to a heating–cooling–heating cycle was tested. During the experiment, it was found that the mechanical strain exhibited a hysteresis during the temperature cycle. Afterwards, finite element simulations were implemented and the hysteresis was successfully reproduced. In addition, the effects of structural parameters such as friction coefficient, clamping force, fastener-hole clearance and bolt spacing on the hysteretic response of thermal stress were revealed.

It can be speculated from the experimental and numerical studies that the relative movement of bolts inside the surrounding holes, together with the contact and friction on the contacting surfaces, are responsible for the hysteresis of thermal stress. The combination of structural parameters that raises the resistance of bolt movement moderately, e.g., higher friction coefficient or larger clamping force, would broaden the temperature range of the hysteretic regime (or nonlinear phase) during which the heating and cooling responses have a lag and enhances the magnitude of thermal stress. If the bolt movement is overly constrained, such as by extremely high friction coefficient or extremely large clamping force or nearly zero clearance, the mechanical strain induced by thermal stress would degrade to essentially linear responses.

The reported work measured the evolution of mechanical strain induced by thermal stress in hybrid structures which are widely used in aerospace and potentially other industries and attempted to provide physical insights on the observed hysteretic response of thermal stress by numerous finite element simulations. The results are helpful for further studies

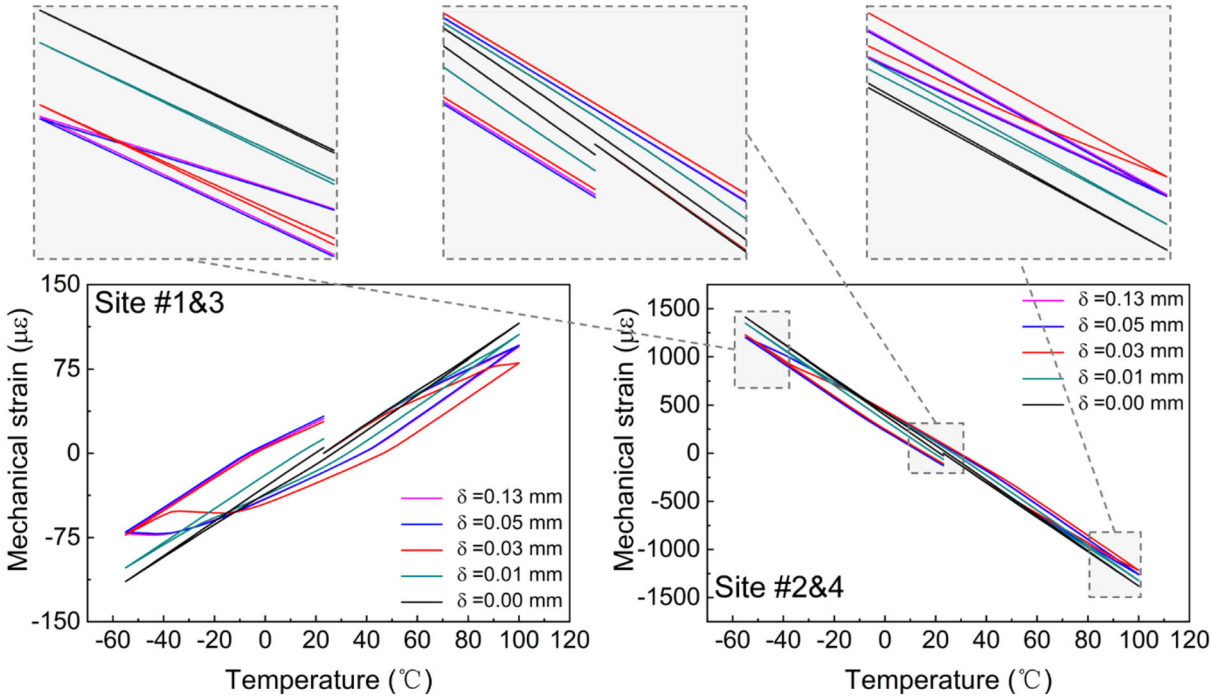

Fig. 10 Mechanical strain variation with temperature for different fastener-hole clearances

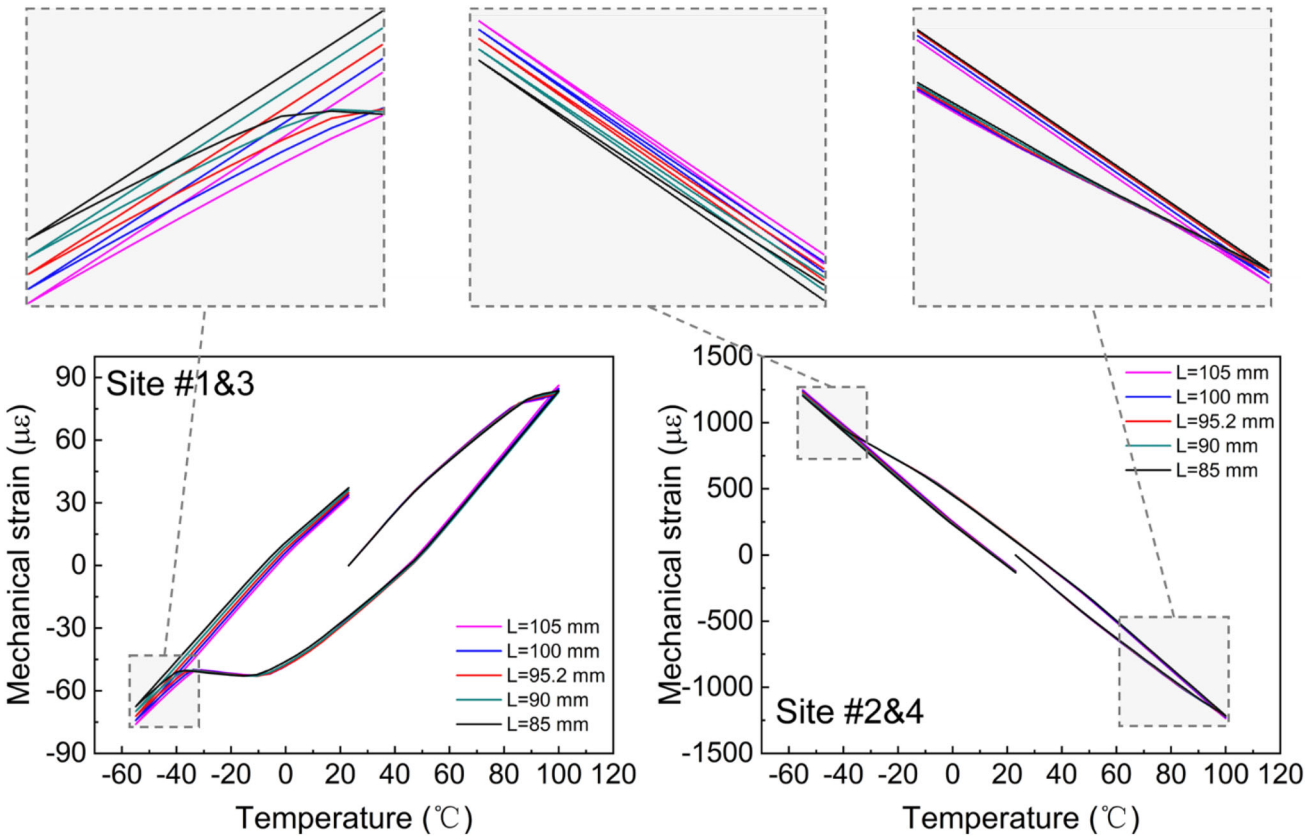

Fig. 11 Mechanical strain variation with temperature for different bolt spacing in specimen

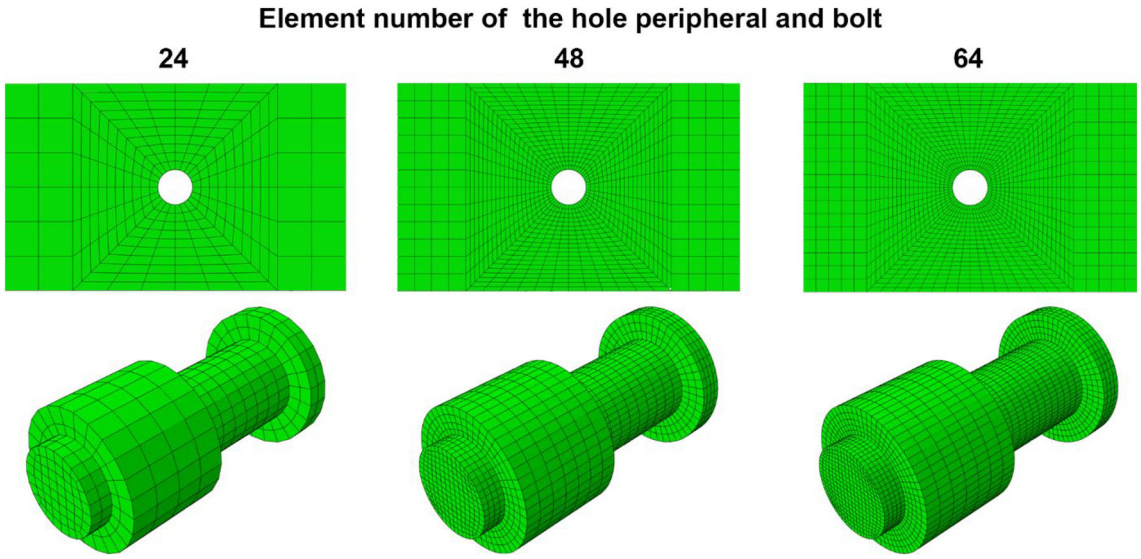

Fig. 12 Mesh density diagram of specimen

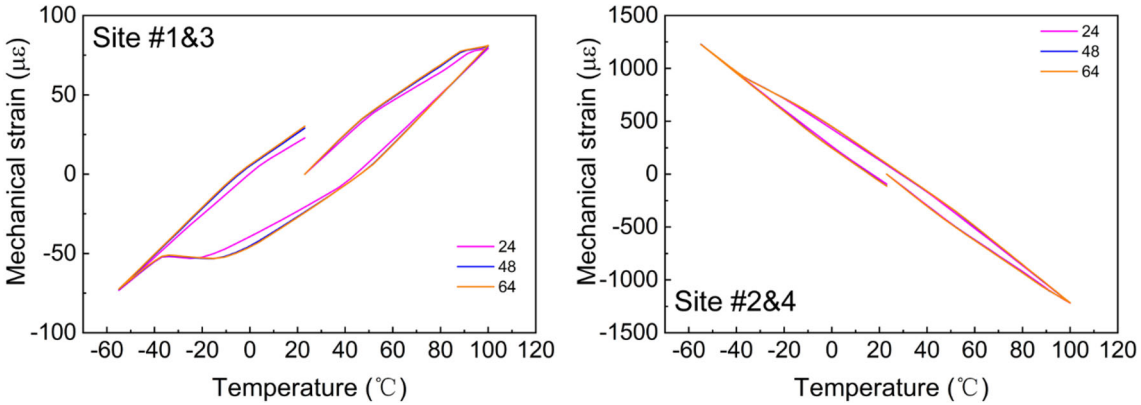

Fig. 13 Comparison of simulation results using the three mesh densities characterized by uniform 24, 48 and 64 elements on the hole peripherals

on the safety of hybrid structures subjected to cyclic thermo-mechanical loads.

Appendix: Mesh sensitivity study

Three mesh densities were employed to run FE simulations to investigate the sensitivity of the simulation results on the mesh. The three meshes have uniformly 24, 48 and 64 elements on hole peripherals, and accordingly there are 6, 12 and 16 elements along the width of the plates in the rectangular regions outside the vicinity of the holes, as shown in Fig. 12, in which the meshes of the bolt correspondent to the three densities are also plotted.

The FE simulations results using the three mesh densities described above are shown in Fig. 13. It is found that as the mesh is refined from 24 to 48 elements on the hole peripherals, the hysteresis has a significant change but further refinement of the mesh density to 64 elements on the hole peripherals does not bring discernible improvement of the predictions. Thus, the mesh density with 48 elements on the hole peripherals is selected to serve the FE simulations presented in the paper.

Acknowledgements The authors acknowledge the financial support from National Science Foundation of China (Grant No. 12072199).

Author contributions Conceptualization: Dongjie Jiang; Methodology: Dongjie Jiang; Formal analysis and investigation: Zhiyuan Cong; Writing—original draft preparation: Dongjie Jiang, Zhiyuan Cong; Zhefeng Yu Writing—review and editing: Dongjie Jiang, Zhiyuan Cong; Zhefeng Yu; Funding acquisition: Zhefeng Yu; Resources: Dongjie Jiang; Supervision: Dongjie Jiang.

Funding This work was supported by National Science Foundation of China (Grant No. 12072199).

Data availability The datasets used or analyzed during the present study are available from the corresponding author on reasonable request.

Declarations

Conflict of interest The authors have no competing interests to declare that are relevant to the content of this article.

References

1. Goossens S, de Pauw B, Geernaert T et al (2019) Aerospace-grade surface mounted optical fibre strain sensor for structural health monitoring on composite structures evaluated against in-flight conditions. Smart Mater Struct 28(6):065008
2. Starikov R, Schn J (2001) Quasi-static behaviour of composite joints with protruding-head bolts. Compos Struct 51(4):411–425
3. McCarthy M (2003) BOJCAS: bolted joints in composite aircraft structures. Air Space Europe 3(3):139–142
4. Cai Q, Zhao Q (2021) Effects of temperature and clearance fit on the load distribution of composite-metal hybrid structures. Acta Mater Compos Sin 38(12):4228–4238
5. Fox DE, Swaim KW (1999) Static strength characteristics of mechanically fastened composite joints. NASA/TM-1999-209735
6. Yang C, Sun W, Seneviratne W et al (1971) Thermally induced loads of fastened hybrid composite/aluminum structures. J Aircr 45(2):569–580
7. Deng W, Cheng Z, Tang H (2020) Thermal stress distribution law of hybrid composite metal structures. Chin J Appl Mech 37(2):550–557
8. Hong W, Maoliang Z, Ruijuan F (2015) Finite element analysis on thermal stress of the connection structure between composite and metal sheet. Aeronaut Sci Technol 16(1):17–31
9. Abdus S, Cheng X, Huang W et al (2019) Bearing failure and influence factors analysis of metal-to-composite bolted joints at high temperature. J Braz Soc Mech Sci Eng 41(7):298
10. Liu Z, Qing G (2019) A progressive damage model introducing temperature field for bolted composite joint with preload. Modell Simul Mater Sci Eng 27(6):065011
11. Soykok IF, Sayman O, Ozen M et al (2013) Failure analysis of mechanically fastened glass fiber/epoxy composite joints under thermal effects. Compos B Eng 45(1):192–199
12. Turvey GJ, Sana A (2016) Pultruded GFRP double-lap single-bolt tension joints—temperature effects on mean and characteristic failure stresses and knock-down factors. Compos Struct 153:624–631
13. Zhu Y, Xiong J (2019) High temperature effect on mechanical performance of screwed CFRC-Ti alloy joints repaired with metal inserts. J Compos Mater. https://doi.org/10.1177/002199832098
14. Norwood DS, Brown KS, Malaznik S et al (2022) A study of airframe thermal stresses in hybrid composite-metallic structure. AIAA SCITECH 2022 Forum
15. Zhu Y, Xiong J (2022) Temperature effect on mechanical performances and failure mechanisms of single-lap countersunk-screwed CFRPI-metal joint. Compos Struct 289:115459
16. Zhu Y, Xiong J, Luo C et al (2021) Progressive damage characteristics of screwed single-lap CFRPI-metal joint subjected to tensile loading at RT and 350°C. J Compos Mater 55:2069–2086
17. Coman C, Constantinescu DM (2019) Temperature effects on joint strength and failure modes of hybrid aluminum–composite countersunk bolted joints. Proc Inst Mech Eng Part L J Mater Design Appl 233:2204–2218
18. Karimi S, Rezvani Nasab M, Afshari R et al (2023) Effect of hygrothermal and thermal aging on the fatigue and static strength of mechanical and hybrid single lap joint. Compos Struct 309:116692
19. Zhu Y, Xiong J (2023) Temperature-moisture-mechanical coupling fatigue behaviours of screwed composite-steel joints. Int J Fatigue 173:107700
20. Cai Y, Zhang Y, Shi X et al (2020) Method of in-situ temperature compensation for resistance strain gauge. Eng J Wuhan Univ 53(7):591–596
21. Landis CM (2003) On the strain saturation conditions for polycrystalline ferroelastic materials. J Appl Mech 70:470–478
22. Landis CM (2002) Fully coupled, multi-axial, symmetric constitutive laws for polycrystalline ferroelectric ceramics. J Mech Phys Solids 50:127–152